JOURNAL OF THE ROYAL SOCIETY Interface

Mechanics of plant fruit hooks

Qiang Chen, Stanislav N. Gorb, Elena Gorb and Nicola Pugno

J. R. Soc. Interface 2013 **10**, 20120913, published 30 January 2013

JOURNAL OF THE ROYAL SOCIETY Interface

rsif.royalsocietypublishing.org

Research

Cite this article: Chen Q, Gorb SN, Gorb E, Pugno N. 2013 Mechanics of plant fruit hooks. J R Soc Interface 10: 20120913.
http://dx.doi.org/10.1098/rsif.2012.0913

Received: 6 November 2012
Accepted: 7 January 2013

Subject Areas:
biomechanics, biomaterials

Keywords:
plant hooks, force–displacement curves, Young's modulus, Velcro

Author for correspondence:
Nicola Pugno
e-mail: nicola.pugno@unitn.it

Royal Society Publishing
Informing the science of the future

Mechanics of plant fruit hooks

Qiang Chen[1], Stanislav N. Gorb[2], Elena Gorb[2] and Nicola Pugno[3]

[1]Laboratory of Biomechanics, School of Biological Science and Medical Engineering, Southeast University, 210096 Nanjing, People's Republic of China
[2]Functional Morphology and Biomechanics, University of Kiel, Am Botanischen Garten 1-9, 24098 Kiel, Germany
[3]Department of Civil, Environmental and Mechanical Engineering, University of Trento, 38123 Trento, Italy

Hook-like surface structures, observed in some plant species, play an important role in the process of plant growth and seed dispersal. In this study, we developed an elastic model and further used it to investigate the mechanical behaviour of fruit hooks in four plant species, previously measured in an experimental study. Based on Euler–Bernoulli beam theory, the force–displacement relationship is derived, and its Young's modulus is obtained. The result agrees well with the experimental data. The model aids in understanding the mechanics of hooks, and could be used in the development of new bioinspired Velcro-like materials.

1. Introduction

Recently studied hook-like structures on different plant organs, which enhance their attachment ability, serve two main functions: (i) to support stems in a densely occupied environment [1], and (ii) to interlock with animal fur and feathers for fruit and seed dispersal [2]. To separate hooks from their supports, a large force per unit area has to be applied.

Bauer *et al.* [1] have investigated the structure and mechanical properties of the climbing plant *Galium aparine*, which attaches to host plants using its leaves. In this experimental study, sets of tensile experiments were performed to estimate the contact separation force of single hooks in different load directions. Additionally, sliding friction of leaves was evaluated, to demonstrate difference in frictional properties between hooks situated on *abaxial* and *adaxial* sides of leaves. The authors found that differences in the hook position on the leaf surface, their orientations, shapes and sizes resulted in variable friction properties and pronounced friction anisotropy of both leaf sides. Owing to this, the plant can hold supports tightly, and thus climb successfully to obtain more sunshine needed for photosynthesis.

On the surface of some fruits and seeds (later called *fruits*), hooks are involved in epizoochorous dispersal [2]. Such fruits can detach easily from their parental plants and attach to animals by interlocking with the animal hair or feathers. Using animals as vectors, they are carried to other places located at distances ranging from tens of metres to tens of kilometres [3,4] from the parent plant. The dispersal distance depends on the particular animal vector, hook geometry, density of hooks, properties of hook material and fruit mass. With such interesting phenomenon, recently, mechanical measurements on single hooks of *Geum urbanum*, *Agrimonia eupatoria*, *Ga. aparine* and *Circea lutetiana* were carried out [2] (figure 1). It was revealed that the hook size and shape had a great influence on the contact separation force, generated by hooks during interlocking.

However, addressing how the material properties of fruit hooks influence their mechanical behaviour, the relationship between them was not defined quantitatively in theory. In this study, we developed a geometrical model aiming at prediction of mechanical behaviours of the hooks. First, the entire hook geometry is subdivided into two parts; for each part, geometry was simplified and determined by several parameters taken from Gorb & Gorb [2]. Second, Euler–Bernoulli beam theory was used to derive the force–displacement relationship and to predict Young's moduli of hook materials, which describes hook materials' stiffness and is an important parameter in the design of man-made hook fastener materials.

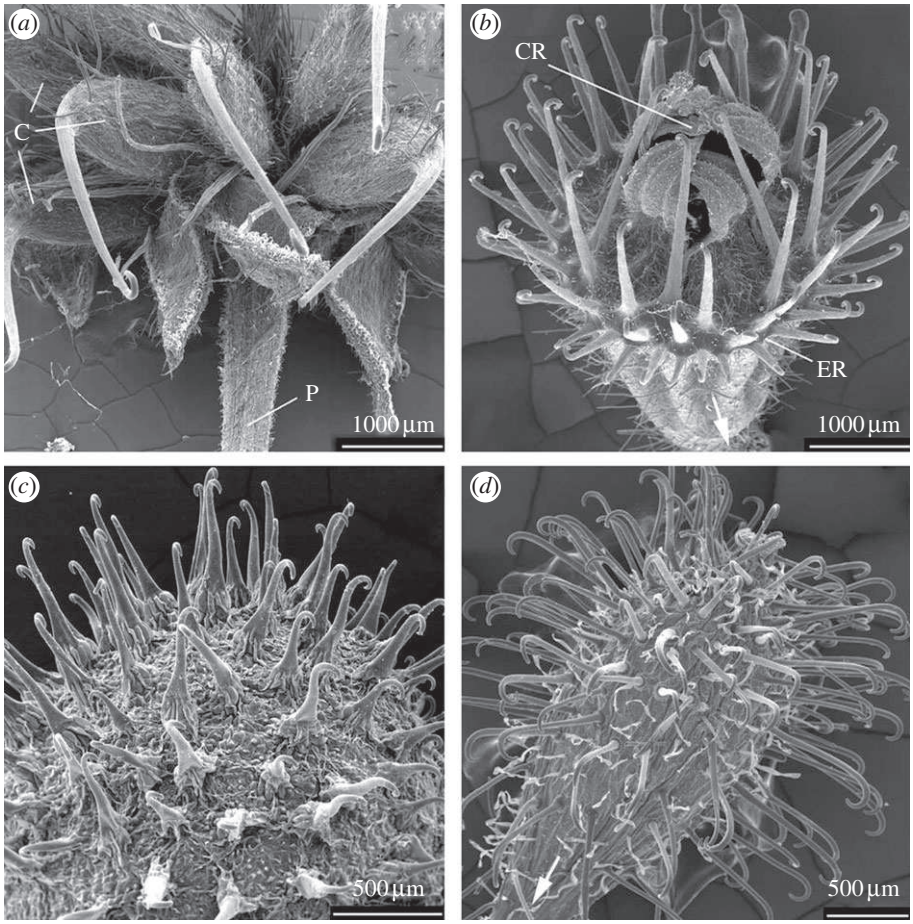

Figure 1. Fruit hooks of four plant species: (*a*) *Ge. urbanum;* (*b*) *A. eupatoria;* (*c*) *Ga. aparine* and (*d*) *C. lutetiana*. Reprinted with permission from Gorb & Gorb [2] (Copyright 2002 Elsevier).

2. Mechanical measurements on single hooks

2.1. Geometrical description of hooks

Fruits of *A. eupatoria*, *C. lutetiana*, *Ga. aparine* and *Ge. urbanum* were collected in Tübingen (Germany), and examined using a light microscopy (Mitutoyo MF U-510 TH) in order to quantify the geometrical parameters of the hooks, such as the total hook length (*ls*), the diameter in basal (*db*) and distal parts (*dd*) of a nearly straight rod part, the diameter (*dh*) and length (*lh*) of a curved part as well as its span (*sh*). These parameters, together with the hook number per fruit, are reported in table 1 (data from Gorb & Gorb [2]).

2.2. Testing method and results

To study the mechanical properties of fruit hooks, experiments were conducted with individual hooks of each plant species. A single hook was cut off from the fresh fruits, and its basal part was glued to a platform P using universal glue GL (figure 2). The upper (curved) part of the hook was interlocked to a steel-wire loop LP with a diameter of 50 µm, which was attached to a glass spring G with a spring constant of 290 N m^{-1}. The hook slowly moved down driven by a motor on a force tester (Tetra GmbH, Ilmenau, Germany) during the experimental process until the contact between the hook and the loop was broken. The force tester included three main parts, a platform P, a glass spring G and a fibre optical sensor FOS, which monitored the spring deflection by a mirror M, and was connected to a computer used for data acquisition (figure 2). The recorded force–displacement curves are presented in figure 3 (data from Gorb & Gorb [2]).

It is found that the displacement is very large compared with the overall hook length. On the one hand, when the hook is subjected to a force, the pulling-straight effect contributes to the large deformation. On the other hand, because hook samples contain some residual water, their mechanical behaviours are rather ductile, thus, their deformations are large compared with the hooks' size. As for the sliding of the metal hook during testing, it has weak influence on the results obtained, because we have used only the linear part of the force–displacement curve.

Additionally, the number of burrs per fruit is in the approximate range from 73 for *A. eupatoria* to 183 for *Ga. aparine* (table 1); thus, if the twist between hooks and animal hairs, which improves their interlocking effects, is not considered, then the force required to detach a fruit from an animal is from 646.1 mN for *C. lutetiana* to 4511.4 mN for *A. eupatoria* according to the breaking force in figure 3. The detaching force is much larger than the fruits' mass [2]. In biological sense, the dispersal distance relying on different hook geometry, density of hooks and properties of hook materials seems to be illustrated, even though the relevant data are still unavailable.

3. Geometrical model of the hook

We used combinational curves to construct the hook model (figure 4*a*), according to the scanning electronic microscope

Table 1. Geometrical parameters of hooks in four plant species (data from Gorb & Gorb [2]). *n* denotes the number of hook samples.

	Agrimonia eupatoria			*Circea luteriana*			*Galium aparine*			*Geum urbanum*		
geometrical parameters	mean	s.d.	*n*	mean	s.d.	*n*	mean	s.d.	*n*	mean	s.d.	*n*
ls (µm)	1845.9	408.3	20	1066.1	272.8	20	281.1	42.1	20	4654.6	369.8	20
lh (µm)	94.3	13.3	20	87.2	40.9	20	19.6	4.8	20	235.0	34.1	20
dh (µm)	64.2	11.1	20	46.6	16.2	20	9.8	2.6	20	96.7	8.7	20
sh (µm)	90.9	20.9	20	173.6	60.3	20	29.6	11.8	20	220.3	29.0	20
dd (µm)	67.8	10.1	20	57.7	19.2	20	11.2	2.3	20	97.6	7.5	20
db (µm)	169.2	64.6	20	83.0	26.4	20	45.1	8.3	20	298.4	56.6	20
hooks per fruit	73.7	10.2	10	182.1	24.7	6	183.3	27.2	8	1	0	50

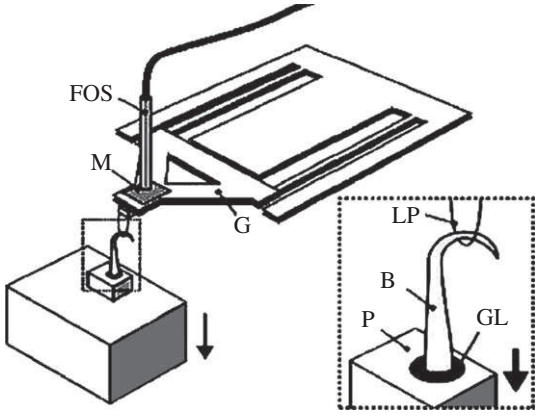

Figure 2. Schematic of force tester. B, FOS G, GL, LP, M and P indicate hook, fibre optical sensor, glass spring, glue, steel-wire loop, mirror and platform, respectively. Reprinted with permission from Gorb & Gorb [2] (Copyright 2002 Elsevier).

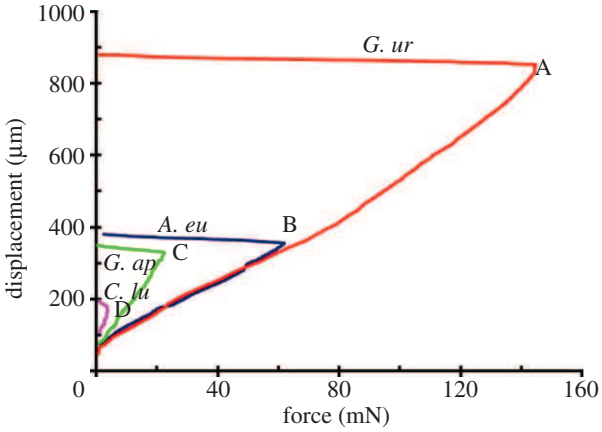

Figure 3. Force–displacement curves measures for single hooks of four plant species. Data from Gorb & Gorb [2]. A, B, C and D are separation points of the hooks, when the critical forces arrive. *A. eu, C. lu, G. ap, G. ur* indicate *Agrimonia eupatoria, Circea lutetiana, Galium aparine, Geum urbanum*, respectively. (Online version in colour.)

images in figure 1. The model is considered as a combination of two parts: a trapezoid cylinder with upper diameter *dd*, and lower diameter *db* and a semicircle on the top (figure 4*a*). The plane section of the semicircle is composed of three circles sharing a centre *O*, and their radii are denoted by R_1, R_2, R_3, respectively. The radii are determined by the hook span *sh* and the upper diameter *dd*, i.e. $R_1 = \frac{1}{2}(sh - \frac{1}{2}dd)$, $R_2 = \frac{1}{2}(sh + \frac{1}{2}dd)$ and $R_3 = \frac{1}{2}(sh + \frac{3}{2}dd)$. Here, we do not consider *lh* and *dh* in determining the radii, but they are used to calculated the length of the trapezoid cylinder, i.e. $ls - lh - dh$, where *lh* and *dh* are hook length and diameter of the middle part in the semicircle, respectively. Based on the model, we derive two important parameters by geometrical analyses, i.e. the cross-sectional radii of the two parts that determine the cross-sectional properties, e.g. moment of inertia. For the trapezoid cylinder, the radius is expressed as $r_1(y) = (dd/2)(1 + Py)$ with $P = (1 - db/dd)/(ls - lh - dh)$. For the semicircle, we assume that cross sections are uniform with a diameter *dd*; thus, we derive the following radius: $r_2(\theta) = dd/2$. Using our basic model of hooks and mean geometrical parameters listed in table 1, the four geometrical models for hooks of the four plant species can be obtained.

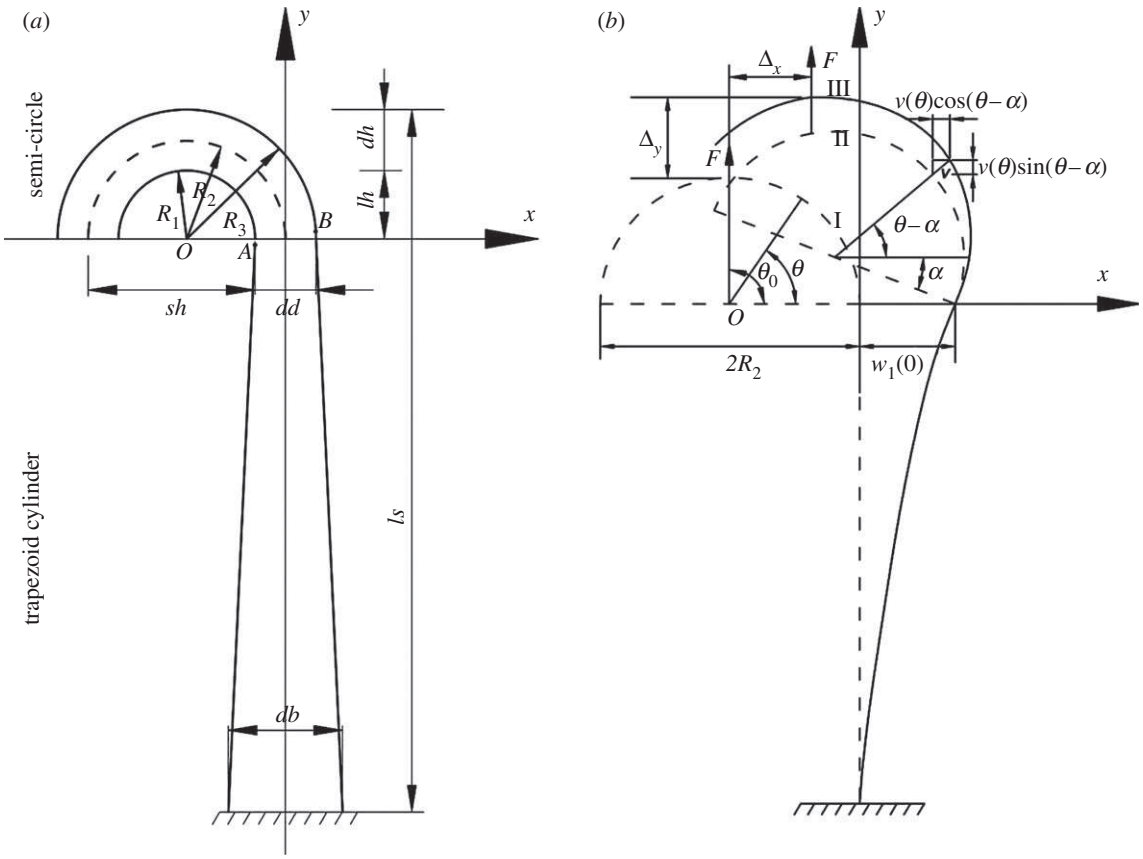

Figure 4. Schematic of hooks. (*a*) Geometrical model. (*b*) Deformation under tensile load. See §§2.1 and 3 for abbreviations in (*a*) and §5 for abbreviations in (*b*).

4. Displacement of the hook

If the interaction between the hook and animal hair or feather is strong, then fruits could be dropped at a more remote place. The information on the mechanical properties of hook materials is necessary to better understand the underlying dispersal mechanism. In the following sections, the Euler–Bernoulli beam theory was used to calculate hook mechanics.

4.1. Trapezoid cylinder part

For the trapezoid cylinder part (figure 4*a*), the displacement includes the axial displacement $u_1(y)$, induced by the axial force F, which contacts with the top of the inner semicircle with radius R_1. The horizontal displacement $w_1(y)$ is imposed by the bending moment $M_1(y) = -FR_2$, which is considered as a constant during the hook deformation. By neglecting the axial compliance and thus displacement $u_1(y)$, the displacement $w_1(y)$ must satisfy the classical elastic line equation:

$$\frac{d^2w_1(y)}{dy^2} = -\frac{M_1(y)}{EI(y)} = \frac{4FR_2}{\pi E}\cdot\frac{1}{r_1(y)^4}. \tag{4.1}$$

Substituting $r_1(y)$ into equation (4.1) and integrating it with boundary conditions $w_1'(-(ls-lh-dh)) = 0$, $w_1(-(ls-lh-dh)) = 0$, we have

$$\left.\begin{aligned} w_1'(y) &= -\frac{64FR_2}{3\pi EPdd^4}\cdot\left[\frac{1}{(1+Py)^3} - \left(\frac{dd}{db}\right)^3\right] \\ \text{and}\quad w_1(y) &= -\frac{32FR_2}{3\pi EP^2dd^4} \\ &\quad\cdot\left[-\frac{1}{(1+Py)^2} - 2\left(\frac{dd}{db}\right)^3(1+Py) + 3\left(\frac{dd}{db}\right)^2\right]. \end{aligned}\right\} \tag{4.2}$$

In the case of $y = 0$, we can find the rotation angle $\alpha = w_1'(0)$ and the horizontal displacement $w_1(0)$ at the distal end, i.e.

$$\alpha = w_1'(0) = -\frac{64FR_2}{3\pi EPdd^4}\cdot\left[1 - \left(\frac{dd}{db}\right)^3\right]$$

and

$$w_1(0) = -\frac{32FR_2}{3\pi EP^2dd^4}\cdot\left[-1 + 3\left(\frac{dd}{db}\right)^2 - 2\left(\frac{dd}{db}\right)^3\right].$$

4.2. Semicircle part

In this part (figure 4*a*), we decompose the displacement into two steps: one is the rigid displacement, caused by both the rotation and translation of the distal end, and the other one is deformation displacement (figure 4*b*). Note that the displacement trajectory of the hook tip resembles the centroid line (dashed line in figure 4*a*).

4.2.1. Rigid movement

In the case of rigid movement, the semicircle moves to position II from its original position I. In position II, the coordinate vector of the semicircle is expressed as

$$\boldsymbol{r}_{\mathrm{II}} = N\boldsymbol{r}_{\mathrm{I}} + \boldsymbol{w}_1, \tag{4.3}$$

with

$$N = \begin{bmatrix} \cos\alpha & \sin\alpha \\ -\sin\alpha & \cos\alpha \end{bmatrix},$$

$$\boldsymbol{r}_I = (-R_2 + R_2\cos\theta, R_2\sin\theta)^{\mathrm{T}}$$

and

$$\boldsymbol{w}_1 = (w_1(0), 0)^{\mathrm{T}},$$

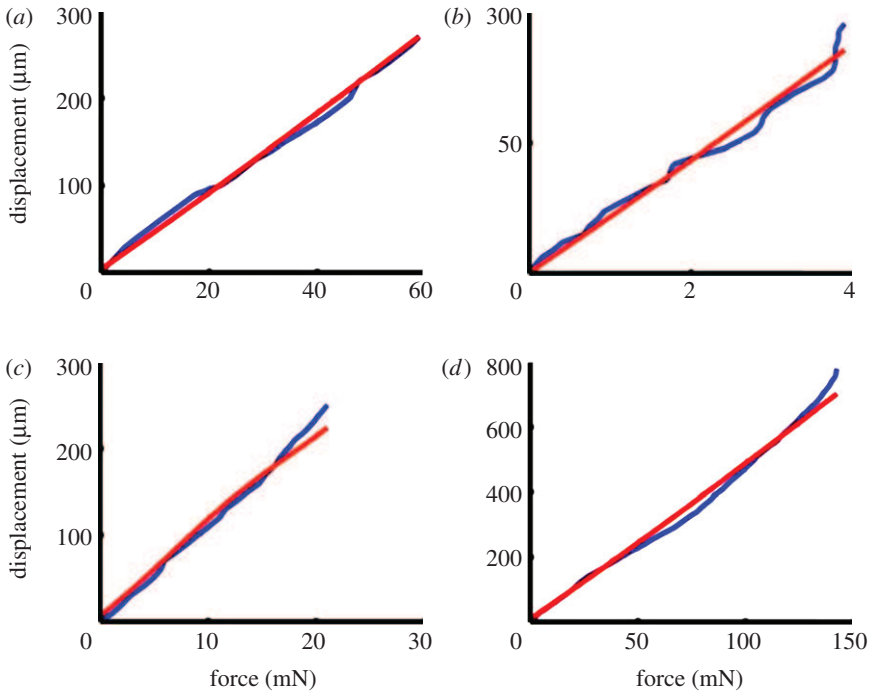

Figure 5. (*a–d*) Comparison between experimental and theoretical force–displacement curves for hooks of the four plant species. Red lines are theoretical results. Blue lines are experimental results. (*a*) *A. eupatoria*, (*b*) *C. lutetiana*, (*c*) *Ga. aparine*, (*d*) *Ge. urbanum*. Data from Gorb & Gorb [2]. (Online version in colour.)

where $\boldsymbol{r}_{\mathrm{I}}$ is the original position vector, $\boldsymbol{w}_1$ is the translational vector of the coordinate transformation, N is the rotation matrix of the coordinate transformation. Correspondingly, due to the rigid movement, the point, on which the applied force F acts, maintains the same rotation angle α from its original position: at the beginning, the force F acts on the semicircle at the point with an angle coordinate of $\theta_0 = 90^\circ$, and the coordinate vector is expressed as $(X_0, Y_0) = (-R_2 + R_2 \cos\theta_0, R_2 \sin\theta_0)$.

4.2.2. Deformation displacement

The displacement $v(\theta)$ can be calculated in the same way as that in §4.1, but the coordinate should be replaced by the arc length s, which is the function of θ (i.e. $s = \theta R_2$) as previously suggested in the nonlinear Velcro mechanics [5]. The moment $M_2(\theta)$ acting on the semicircle part is expressed as $M_2(\theta) = -F[\boldsymbol{r}_{\mathrm{II}}(\theta) - \boldsymbol{r}_{\mathrm{II}}(\theta_0 + \alpha)] \cdot \boldsymbol{e}_x$, when $\theta < \theta_0 + \alpha$, where $\boldsymbol{e}_x = (1,0)^{\mathrm{T}}$ is the unit vector along the x-axis. Thus, the displacement is expressed as

$$\frac{d^2v(\theta)}{ds^2} = \frac{d^2v(\theta)}{R_2^2 d\theta^2} = -\frac{M_2(\theta)}{EI(\theta)} = \frac{4FR_2}{\pi E} \cdot \frac{\cos(\theta - \alpha)}{r_2(\theta)^4}. \tag{4.4}$$

Plugging $r_2(\theta)$ into equation (4.4), we obtain

$$\frac{d^2v(\theta)}{d\theta^2} = \frac{64FR_2^3}{\pi E d d^4} \cdot \cos(\theta - \alpha). \tag{4.5}$$

Integrating equation (4.5) with boundary conditions $v'(0) = 0$ and $v(0) = 0$, we obtain the expressions of the cross-section rotation angle and displacement as

$$\left.\begin{aligned} v'(\theta) &= \frac{64FR_2^3}{\pi E d d^4} \cdot [\sin(\theta - \alpha) + \sin\alpha] \\ \text{and} \\ v(\theta) &= \frac{64FR_2^3}{\pi E d d^4} \cdot [-\cos(\theta - \alpha) + \theta \sin\alpha + \cos\alpha]. \end{aligned}\right\} \tag{4.6}$$

Furthermore, the deformation displacement vector is $\boldsymbol{v} = (v(\theta)\cos(\theta - \alpha), v(\theta)\sin(\theta - \alpha))^{\mathrm{T}}$. Thus, the final position coordinate of the semicircle part can be determined as

$$\boldsymbol{r}_{\mathrm{III}} = \begin{cases} \boldsymbol{r}_{\mathrm{II}} + \boldsymbol{v}, & \text{if } \theta < \theta_0 + \alpha \\ \boldsymbol{r}_{\mathrm{II}} + \boldsymbol{v}(\theta_0 + \alpha), & \text{if } \theta > \theta_0 + \alpha \end{cases}. \tag{4.7}$$

In particular, for the part $\theta < \theta_0 + \alpha$, the new position in the coordinate is expressed as

$$\begin{cases} X(\theta) = -R_2 \cos\alpha + R_2 \cos(\theta - \alpha) + w_1(0) + v(\theta)\cos(\theta - \alpha) \\ Y(\theta) = R_2 \sin\alpha + R_2 \sin(\theta - \alpha) + v(\theta)\sin(\theta - \alpha). \end{cases} \tag{4.8}$$

5. Force–displacement relationship

By comparing the positions before and after deformation of the points, on which the external force is applied, the total displacement experienced by the force F can be described by two components under the conditions of $\theta_0 = 90^\circ$ and $(X_0, Y_0) = (-R_2 + R_2 \cos\theta_0, R_2 \sin\theta_0)$:

$$\begin{cases} \Delta_x = X(\theta_0 + \alpha) - X_0 = -R_2 \cos\alpha + w_1(0) + R_2 \\ \Delta_y = Y(\theta_0 + \alpha) - Y_0 = R_2 \sin\alpha + v(\theta_0 + \alpha). \end{cases} \tag{5.1}$$

5.1. Comparison between experimental and prediction force–displacement curves

Using equation (5.1), the theoretical force–displacement curves of hooks of the four plant species are obtained by fitting the experimental curves (figure 5). These curves reflect the typical constitutive behaviours of plant hooks. We found that the relationships are almost linear and are consistent with the experimental curves obtained by the same experimental design but used in estimating the ultimate load [6]. From these fits, Young's moduli were predicted (figure 6*a*). By taking the *A. eupatoria* hook as an example, we plotted the deformation, when the external force F equals 20 mN (figure 6*b*).

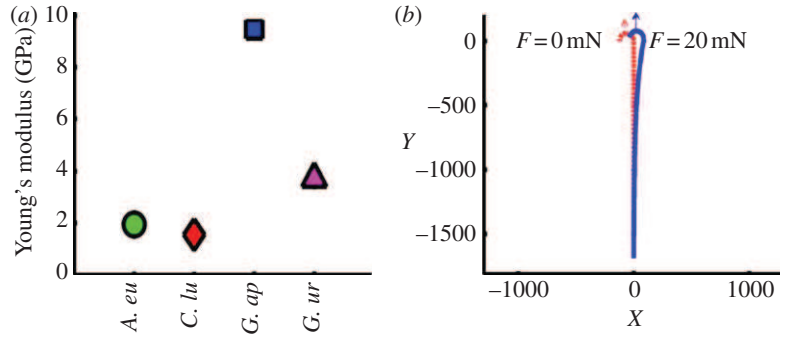

Figure 6. (*a*) Theoretically estimated Young's moduli for different hooks. (*b*) Model of the hook deformation in *Agrimonia eupatoria* at the applied load of $F = 20$ mN. Blue line denotes the deformed configuration of the hook. Red line indicates the initial (not-deformed) configuration of the hook. *A. eu*, *C. lu*, *G. ap*, *G. ur* are *Agrimonia eupatoria, Circea lutetiana, Galium aparine, Geum urbanum*, respectively. (Online version in colour.)

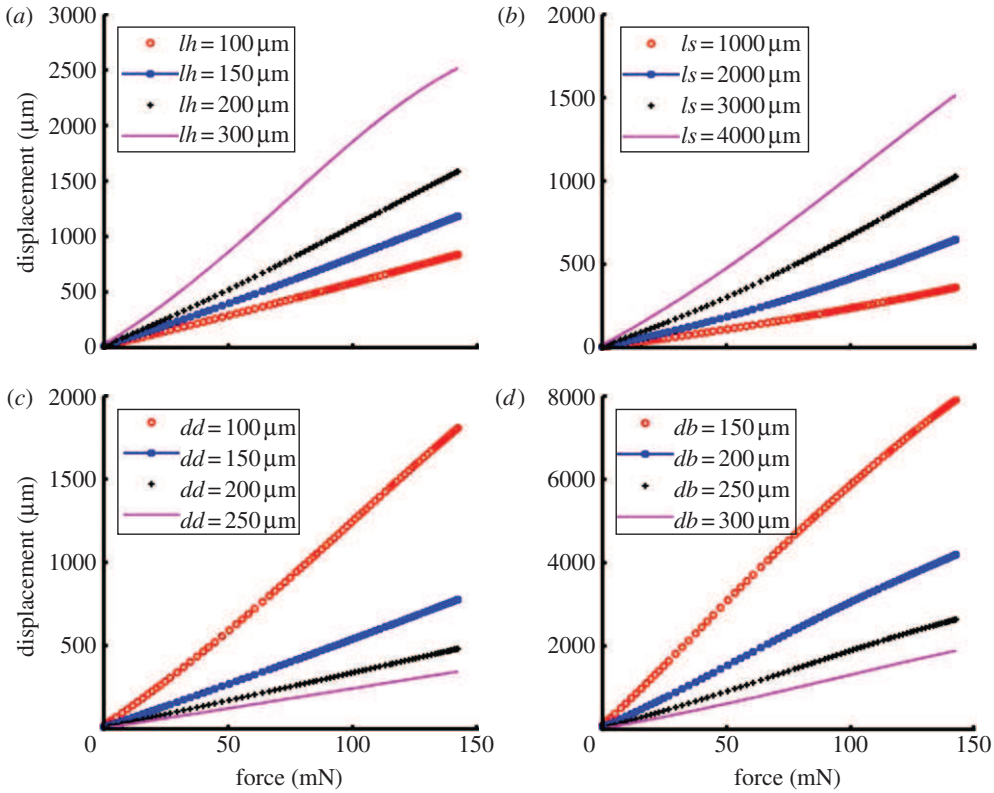

Figure 7. Influences of geometrical parameters on the mechanical behaviour of hooks. (*a*) Influence of *lh*, which reflects the hook span; (*b*) influence of hook length *ls*; (*b*) influence of the diameter in distal end *dd*; (*b*) influence of the diameter in basal end *db*. (Online version in colour.)

Values of Young's moduli obtained for four plant species studies are comparable to those reported for the grass hedge stems (2.6–8.5 GPa) [7], lignin (2.0 GPa) [8] and plant cell wall (7.0–15.0 GPa) [9]. Young's modulus of the *Ga. aparine* hook is the highest (≈9.5 GPa; figure 6*a*) and corresponds well to the range of values 2.02–23.2 GPa, previously calculated for different individual hooks of this plant species [6]. Young's modulus of the *C. luteriana* hook is the lowest among plant species studied (figure 6*a*). This also verifies previous experimental results [2]: although the size of the *Ga. aparine* hooks was the smallest, the load at contact separation was larger than that of *C. luteriana* (figure 3). The latter has a lower material stiffness, which induces a slip off instead of hook fracture observed previously [2]. Compared with *Ga. aparine*, the *Ge. urbanum* hook has a lower Young's modulus (figure 6*a*), but a relative high load at contact separation (figure 3). This may be interpreted by the larger size of *Ge. urbanum* hooks.

5.2 Mechanical behaviours of hooks

It is worth saying that the composite structure and material properties of fruit hooks were previously studied only in *Ga. aparine*. Staining of resin-embedded semithin sections with safranin and fast green showed that the hook wall contains cellulose and lignin [6]. Using force–distance curves obtained in contact separation experiments [2,6], Young's moduli of the hooks with and without a base were calculated in a different way. Moreover, hooks with and without the base showed significantly different values of the elastic moduli: 2.02 GPa and 23.20 GPa, respectively ($H = 755.44$, d.f. $= 1$, $p < 0.001$, Kruskal–Wallis one-way ANOVA on ranks).

Moreover, from the viewpoint of mechanical design, in order to construct a desirable hook-based fastening device, it would be of importance to know how geometrical parameters of hooks influence the mechanical behaviour of hooks independently of the composition of the materials

used. Therefore, we studied four parameters, namely the hook length (*ls*), hook span (*lh*), the diameter in distal end (*dd*) and the diameter in basal end (*db*), respectively, based on the data obtained for *Ge. urbanum* hooks. The results of such an analytical study, where one of the geometrical parameters was varied and the others were kept constant, are reported in figure 7. We can see that increasing hook length (*ls*) and hook span (*lh*) results in a greater displacement under identical external forces, which indicates a more compliant hook; while under identical external forces, increasing the diameter in the distal end (*dd*) and in the basal end (*db*) produces a smaller displacement, which suggests a stiffer hook.

6. Conclusion

We have developed a theoretical model with the aim of explaining the mechanical behaviour of plant hooks and to obtain the force–displacement relationship, degree of hook deformation and Young's modulus. The influences on the mechanical behaviour of hooks are discussed and thus, the present theory can potentially be used for understanding the mechanics of natural hooks and related structures. Additionally, the model could help in designing new bioinspired Velcro-like mechanical adhesives [5,6,10].

The research related to these results has received funding from the European Research Council under the European Union's Seventh Framework Programme (FP7/2007–2013)/ERC grant agreement no. 279985 (ERC StG Ideas 2011 BIHSNAM on 'Bioinspired hierarchical super nanomaterials') to N.P. S.N.G. and E.G. were supported by the German Science Foundation (grant C10 within the DFG SFB 677 'Function by switching' to S.N.G.). This study was partly supported by the SPP 1420 priority programme of the German Science Foundation (DFG) 'Biomimetic materials research: functionality by hierarchical structuring of materials' (project no. GO 995/9-2) to S.G.

References

1. Bauer G, Klein M-C, Gorb SN, Speck T, Voigt D, Gallenmüller F. 2011 Always on the bright side: the climbing mechanism of *Galium aparine*. *Proc. R. Soc. B* **278**, 2233–2239. (doi:10.1098/rspb.2010.2038)
2. Gorb E, Gorb S. 2002 Contact separation force of the fruit burrs in four plant species adapted to dispersal by mechanical interlocking. *Plant Physiol. Biochem.* **40**, 373–381. (doi:10.1016/S0981-9428(02)01381-5)
3. Howe HF, Smallwood J. 1982 Ecology of seed dispersal. *Ann. Rev. Ecol. Syst.* **13**, 201–228. (doi:10.1146/annurev.es.13.110182.001221)
4. Manzano P, Malo JE. 2006 Extreme long-distance seed dispersal via sheep. *Front. Ecol. Environ.* **4**, 244–248. (doi:10.1890/1540-9295(2006)004[0244:ELSDVS]2.0.CO;2)
5. Pugno NM. 2007 Velcro nonlinear mechanics. *Appl. Phys. Lett.* **90**, 121918. (doi:10.1063/1.2715478)
6. Gorb EV, Popov VL, Gorb SN. 2002 Natural hook-and-loop fasteners: anatomy, mechanical properties, and attachment force of the jointed hooks of the *Galium aparine* fruit. In *Design and nature: comparing design in nature with science and engineering* (eds CA Brebbia, LJ Sucharov, P Pascolo), pp. 151–160. Boston, MA: WIT Press.
7. Dunn GH, Dabney SM. 1996 Modulus of elasticity and moment of inertia of grass hedge stems. *Trans. ASAE* **39**, 947–952.
8. Cousions WJ. 1976 Elastic modulus of lignin as related to moisture content. *Wood Sci. Technol.* **10**, 9–17. (doi:10.1007/BF00376380)
9. Tashiro K, Kobayashi M. 1991 Theoretical evaluation of three-dimensional elastic constants of native and regenerated cellulose: role hydrogen bonds. *Polymer* **32**, 1516–1526. (doi:10.1016/0032-3861(91)90435-L)
10. Pugno N. 2008 Spiderman gloves. *Nano Today* **3**, 35–41. (doi:10.1016/S1748-0132(08)70063-X)